V European Conference on Computational Fluid Dynamics
ECCOMAS CFD 2010
J. C. F. Pereira and A. Sequeira (Eds)
Lisbon, Portugal, 14–17 June 2010

RECENT ADVANCES IN FLAME RESPONSE PREDICTION FOR COMBUSTION INSTABILITY MODELLING

Santosh Hemchandra*

* Institute of Aerodynamics, RWTH
Wullnerstrasse 5a, 52062, Aachen, Germany.
e-mail: s.hemchandra@aia.rwth-aachen.de

Key words: Heat release response, Combustion instability, transfer functions

Abstract. *Increasingly stringent regulatory limits imposed on pollutant emissions from systems such as land based gas-turbines, industrial boilers etc., has resulted in the adoption of lean premixed combustion systems. These systems are especially prone to combustion instabilities that are characterized by high amplitude oscillations in combustor pressure that can potentially affect their emission levels, hardware integrity and operation range. A key component of any combustion instability prediction approach involves a description of the interaction of perturbations of various kinds, e.g. acoustic velocity perturbations, turbulence, fuel/air ratio oscillations etc., with an unsteady premixed flame. This paper presents a short review of the most significant advances in the development of modelling approaches for this problem that have been developed over the past decade. Modelling approaches for both velocity coupled and fuel/air ratio coupled mechanisms in the limit of small amplitude fluctuations have been reviewed.*

1 INTRODUCTION

Combustion instabilities cause significant problems in the operation of low-emissions premixed combustion systems. This phenomenon results from a two-way coupling process between unsteady heat release and one or more acoustic modes of the combustor resulting in high amplitude pressure oscillations that can adversely affect performance, pollutant emission levels and hardware integrity. Hence it is essential to develop reduced order modeling techniques that can be used in early stages of the design process to perform stability analyses of lean premixed combustors in order to identify regions within their operating envelope where instabilities can occur.

Prediction of the onset of combustion instabilities in premixed combustion systems requires an accurate description of unsteady heat release processes [1, 2]. Modelling these phenomena requires an understanding of the fundamental processes that cause the heat release rate of a premixed flame to oscillate. This occurs in general due to oscillations in burning area, spatial mass burning rate and heat of reaction caused by imposed perturbations in the combustor flow field. The first of these, i.e. oscillations in the burning area of the flame surface are caused by acoustic velocity fluctuations [3, 4], convected vortical disturbances [5, 6], flame extinction/re-ignition [7] and upstream fuel-air ratio fluctuations [8, 9], in addition, several secondary processes such as flame speed sensitivity to stretch [10, 11] and hydrodynamic instabilities [12] can influence the response of burning area to imposed flow-field perturbations. Thus, in general, the net flame response is a superposition of contributions from the above processes.

In addition to the above processes, the presence of gas expansion across the flame surface causes mutual coupling between the motion of the flame and the flow. Moving boundary problems such as these are challenging to solve analytically. Hence, nearly all theoretical analyses of flame response to acoustic forcing are formulated in the limit of vanishingly small heat release response. While the limitations of such analyses are clear they provide scaling laws that provide valuable insight into the relative importance of the physical mechanisms mentioned above in the generation of overall heat release fluctuations of the flame [13].

The aim of the present paper is to present a review of recent advances in analytical and computational efforts aimed at elucidating the fundamental mechanisms that control heat release rate response. These analyses have been mostly based on the level-set equation approach, first applied to the present problem by Fleifil et al. [3]. The rest of this paper is organized as follows. Section 2 presents a theoretical overview of the problem and discusses the assumptions common to all the analyses presented herein. Section 3 reviews developments in the modeling of velocity coupled response to flow velocity fluctuations. Section 4 reviews developments in modeling efforts for fuel/air ratio coupled response mechanisms. Section 5 concludes the paper and provides an outlook on issues for future investigations.

2 THEORETICAL PRELIMINARIES

All the analyses reviewed in the present paper make the following assumptions.

1. The flame is a thin moving boundary between products and reactants.
2. The heat release across the flame is neglected.

The first assumption implies that all the flow length scales are larger than the flame thickness. This assumption has been shown to be valid in numerous experimental studies of self-excited

combustion instabilities in premixed flame combustors (see for eg. [13, 14]). Thus, the instantaneous flame surface motions can be tracked using the G-equation [15].

$$\frac{\partial G}{\partial t} + \vec{u} \bullet \nabla G = s_L \left| \nabla G \right| \tag{1}$$

Where, $\vec{u}$ is the flow velocity and s_L is the local laminar flame speed. The function G is defined in general as follows,

$$G(\vec{x},t) = \begin{cases} G < G_o & \vec{x} \text{ in reactants} \\ G = G_o & \vec{x} \text{ on the flame} \\ G > G_o & \vec{x} \text{ in products} \end{cases} \tag{2}$$

Thus, the instantaneous flame location is tracked as a level-set of the scalar field *G*. This equation has been the central starting point for several approaches to modeling premixed combustion [15, 16].

The second assumption above is more restrictive. The implication here is that the flow field in the combustor is unaffected by the upstream flow. This however, is not true in practice as the flame modifies both the mean and perturbation components of the approach flow due to reflection and refraction of acoustic waves and flame front instabilities. Thus, in general, a rigorous analytical approach to solving for the dynamics of the flame surface would involve solving governing equations for the flow field both upstream and downstream of the flame front coupled with proper matching conditions for change in flow variables across the flame surface to account for the effect of gas expansion. This is however, a challenging proposition in all but simple canonical configurations such as flat freely propagating premixed flames (see for e.g. Matalon and Matkowsky [17]). As such, nearly all theoretical analyses of premixed flame heat release response in the past two decades have neglected the influence of temperature jump across the flame (e.g. see [2-6]). Thus, these analyses are rigorously valid in the limit of flames with vanishingly small heat release (e.g. flames in vitiated air in aircraft engine afterburners). Even so, such analyses provide qualitative insight into the influence of various types of perturbations on heat release response in the large heat release case as well. They also allow for a first-cut estimate of instability frequencies and limit cycle amplitudes from reduced order linear acoustic modeling approaches via a describing function analysis [2].

The instantaneous heat release rate from the flame can be written as follows,

$$q(t) = \int_{flame} \rho s_L h_R dA \tag{3}$$

Where, the integral on the RHS is performed over the instantaneous flame surface. It is clear from the above that heat release oscillations can arise due to fluctuations in flame speed, heat of reaction, and burning area. Mechanisms that cause each of these will now be described in turn below.

Consider first, oscillations in combustor flow velocity. These disturbances cause heat release fluctuations in a variety of ways. As noted by Clanet et al[18], these can be classified into categories based on whether they modify the internal flame structure or it geometrical properties. The former category is generally associated with velocity fluctuations whose wavelengths are comparable to the thickness of the premixed flame structure, caused by high frequency pressure oscillations. Such oscillations disturb the internal thermodiffusive balance in the flame structure causing modulations in the local laminar flame speed and reactant flow density resulting in overall heat release oscillations [19-21]. The latter category is associated with large coherent

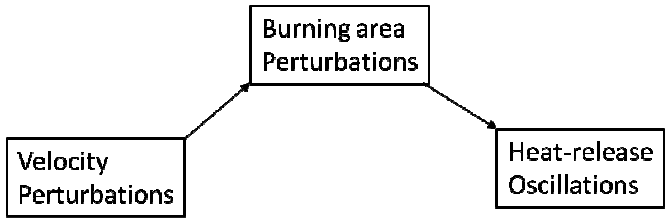

Figure 1: Schematic of velocity coupled heat release oscillation mechanism ($s_L = const.$).

vortical structures that result from the unsteady roll-up of shear layers in the flow caused by acoustic forcing [22].

Fundamentally, flow-field oscillations cause the mass burning rate of reactants entering the flame to fluctuate. These fluctuations are due to both velocity oscillations as well as density oscillations which affect the mass of reactive mixture per unit volume. Further, the position and orientation of the local flame surface depends on the local flow and flame speed characteristics. Thus, velocity perturbations can potentially cause the flame surface to wrinkle, causing the net burning area and hence the heat release rate to oscillate. This mechanism has been extensively studied by several groups and can be represented schematically as shown in fig. 1.

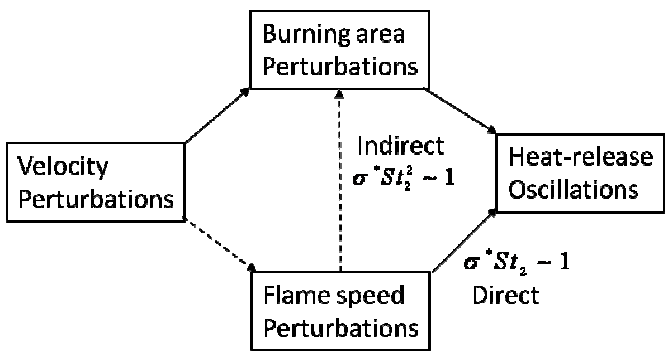

Figure 2: Schematic of velocity coupled heat release oscillation mechanism (s_L depends on stretch). Broken arrows show indirect influence pathways.

Next, unsteady wrinkling causes the local flame speed to vary due to the influence of flame stretch. As such, this influences the net release response of the flame through two additional pathways as summarized in fig. 2. First, unsteady spatial variations in flame speed influences the flame wrinkling process which in turn influences burning area response and hence heat release response. This mechanism is called the indirect stretch influence because the heat release oscillation is modified through the influence of stretch on flame surface kinematics. Next, spatial variations in s_L also cause the spatial variation of local mass burning rate to oscillate in an unsteady manner resulting in heat release oscillations. This mechanism is called the direct stretch response because it represents a source of unsteadiness in heat release that is distinct from burning area oscillations. The influence of flame stretch on heat release response has been studied extensively in the zero heat release limit by Wang et al [10] and Preetham et al [11]. These analyses suggest that the influence of the indirect mechanism becomes significant when $\sigma^* St_2^2 \sim 1$ and the direct mechanism when $\sigma^* St_2 \sim 1$, where, σ^* is a scaled Markstein length and St_2 is a Strouhal number that compares the time taken by a wrinkle to traverse the flame surface with the acoustic time period.

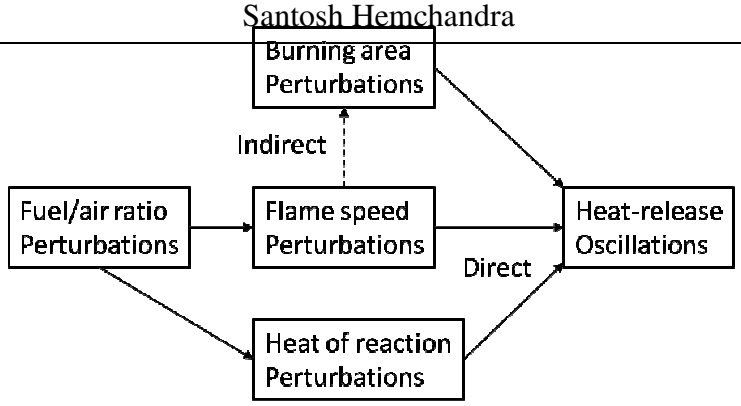

Figure 3: Schematic of fuel-air ratio coupled heat release oscillation mechanism (s_L depends on stretch). Broken arrows show indirect influence pathways.

A third mechanism that causes unsteadiness in heat release oscillations is the response of flames to fuel/air ratio fluctuations. This mechanism has been computationally studied (refs). Further, several reduced order models have been developed and incorporated into acoustic stability analyses of combustion systems. The mechanisms that cause heat-release response oscillations due to perturbations in fuel/air ratio are summarized in fig. 3. Fundamentally, fuel/air ratio oscillations result in fluctuation of the local value of s_L and heat of reaction, h_R. The former influences heat release oscillations via direct and indirect pathways as before. The latter, heat of reaction oscillations directly influence heat release response by changing the local chemical energy content per unit volume at the flame surface. Extensive modeling studies of this response mechanism may be found in Cho and Lieuwen[8] and Hemchandra et al.[23]. Recently, Shreekrishna et al [24] have extended the latter analysis to include non-quasisteady diffusion effects within the preheat zone of the flame as well as the influence of flame stretch on heat response to equivalence ratio mechanisms.

In general, heat release oscillations can occur due to a combination of both of the above two mechanisms. Thus the net heat release response of a flame is the resultant of a superposition of the various pathways described above as summarized schematically in fig. 4. In the limit of small

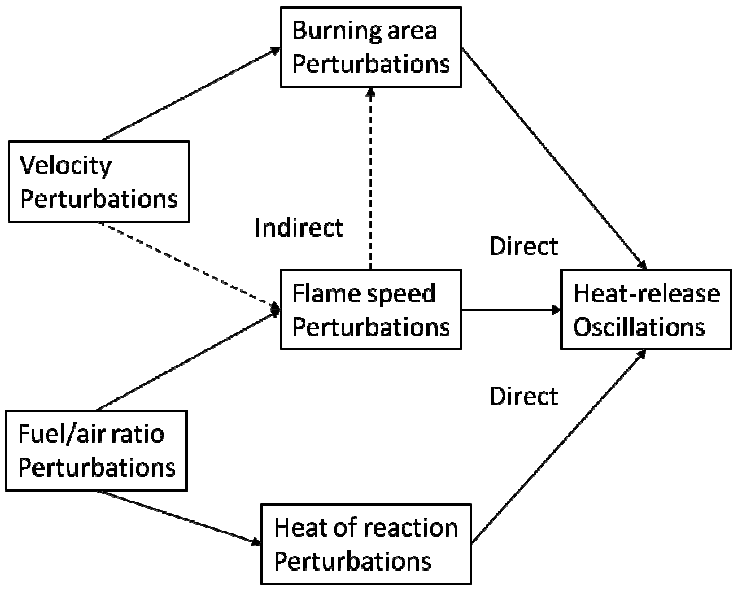

Figure 4: Schematic of heat release oscillation mechanisms due to both velocity-coupled and fuel-air ratio coupled mechanisms (s_L depends on stretch). Broken arrows show indirect influence pathways.

amplitude perturbations, this can be seen quantitatively from a linearized form of eq. as follows,

$$\frac{q'}{q_o} = \frac{A'}{A_o} + \frac{\int_{flame} s'_L dA_o}{\int_{flame} s_{L_o} dA_o} + \frac{\int_{flame} h'_R dA}{\int_{flame} h_{R_o} dA_o} + \frac{\int_{flame} \rho' dA_o}{\rho_o A} \tag{4}$$

Where the superscript, prime, and subscript, 'o', represent the perturbation and mean values of each of the respective quantitites. Each of the terms on the LHS can now be identified with each of the above pathways discussed above, e.g. the pathways shown in fig. 2 quantitatively influence the contributions to the total heat release from the first and second terms on the RHS of eq. . Similarly, the pathways in the fuel-air ratio mechanism would influence the first three terms on the RHS. Also, in this linear limit, the heat release oscillation is characterized by the corresponding transfer functions due to velocity and equivalence ratio (ϕ) perturbations, defined as functions of the excitation circular frequency (ω) as follows,

$$\frac{\hat{q}'(\omega)}{q_o} = F_u(\omega)\frac{u'}{U_o} + F_\phi(\omega)\frac{\phi'}{\phi_o} \tag{5}$$

Thus, the functions F_u and F_ϕ capture the influence of the various heat-release oscillation generating mechanisms via the pathways shown in figs. 2 and 3 respectively. The corresponding perturbation amplitudes on the RHS of eq. (5) represent appropriately chosen reference values that characterize flow and fuel/air ratio perturbations.

A third mechanism that can cause heat release oscillations is the pressure coupled mechanism which captures the influence of an oscillating acoustic pressure field on the net heat release response of the flame (refs). This mechanism is significant when the length scale of pressure oscillations is comparable to that of the flame thickness, i.e. at very large frequencies. In this limit, the flame becomes acoustically non-compact rendering assumption 1 made above invalid (Shreekrishna and Lieuwen [25]). Subsequent analysis of flame response in this limit requires a more complicated approach based on matched asymptotic expansions [19, 26]. These analyses are however not easily generalized to attached flames of technological interest. As such, this paper limits itself to a review of models developed for velocity and fuel/air ratio coupled response in the linear low perturbation amplitude limit.

3 VELOCITY COUPLED RESPONSE

The first attempt at modeling the response of a premixed flame to velocity perturbations using the *G*-equation approach was presented by Fleifil et al.[3] Subsequent groups have extended this original approach in several ways to include effects of flame lift-off [2], axially convected velocity perturbations [5, 6], inflow turbulence [27] and flame stretch [10, 11]. For the purposes of the present discussion, the analysis for an axis-symmetric inverted conical flame base on the development of Preetham et al [6] will be presented. The investigated geometry is shown schematically in fig. 5. The location of the flame at any given radial location is given by $\zeta(r,t)$.

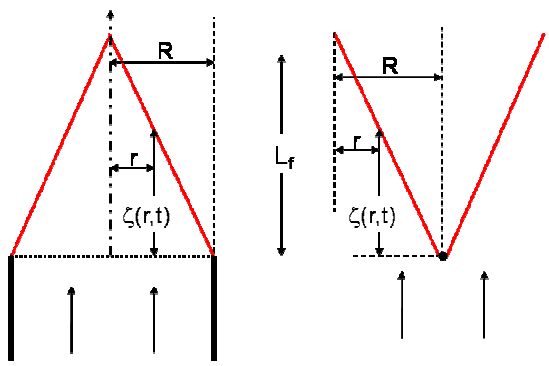

Figure 5: Illustration of conical (left) and inverted wedge (right) shaped flames stabilized on a bluff body. Flow direction is upwards (courtesy Preetham et al [6]).

As such, the function $G(r,z,t) = z - \zeta(r,t)$ satisfies eq. for $G_o = 0$. As such, using this function in eq. yields,

$$\frac{\partial \zeta}{\partial t} + u\frac{\partial \zeta}{\partial r} - v = s_L\sqrt{1+\left(\frac{\partial \zeta}{\partial r}\right)^2} \tag{6}$$

Where, u and v are flow velocity components in the radial and axial directions respectively. The implicit assumption in eq. is that the flame surface remains a single valued function of r at all times. It will also be assumed for the present that s_L is constant and equal to its unstretched value. Next, the radial co-ordinate is normalized by r, the flame surface location by L_f and velocities by the mean flow velocity U_o yields eq. in non-dimensional form as follows ($\beta = L_f / R$),

$$\frac{\partial \zeta}{\partial t} + \beta u\frac{\partial \zeta}{\partial r} - v = \sqrt{\frac{1+\beta^2\left(\frac{\partial \zeta}{\partial r}\right)^2}{1+\beta^2}} \tag{7}$$

Next, the velocities u and v can in general be written in terms of a mean and perturbation value as follows,

$$\begin{aligned} u(r,\zeta,t) &= \varepsilon f_u(r,\zeta,t) \\ v(r,\zeta,t) &= 1+\varepsilon f_v(r,\zeta,t) \end{aligned} \tag{8}$$

Where, the parameter ε characterizes the velocity perturbation amplitude. The functions f_u and f_v represent the spatio temporal structure of the imposed perturbations. Thus, it is possible to find solutions of eq. for small ε as the leading order term in an asymptotic expansion for ζ in terms of ε: $\zeta(r,t) = \zeta_o(r) + \varepsilon\zeta_1(r,t) + O(\varepsilon^2)$. Thus the governing equation for the leading order term can be written as follows,

$$\frac{\partial \zeta_1}{\partial t} - \frac{\beta^2}{1+\beta^2}\frac{\partial \zeta_1}{\partial r} = f_v(r,\zeta,t) - \beta f_u(r,\zeta_o,t)\frac{d\zeta_o}{dr} \tag{9}$$

Further, assuming an attached flame yields the boundary condition,

$$\zeta_1(r=0,t) = 0 \tag{10}$$

Next, the instantaneous heat release rate normalized by its mean value under the present assumptions can be written as follows,

$$q(t)=\frac{\int_0^1 (1-r)\sqrt{1+\beta^2\left(\frac{\partial\zeta}{\partial r}\right)^2}\,dr}{\int_0^1 (1-r)\sqrt{1+\beta^2\left(\frac{d\zeta_o}{dr}\right)^2}\,dr} \tag{11}$$

Finally, the heat release response to leading order can be obtained from eq. as follows,

$$q(t)=1+\varepsilon\frac{\int_0^1 (1-r)\left\{\beta^2\left(d\zeta_o/dr\right)\Big/\sqrt{1+\beta^2\left(d\zeta_o/dr\right)^2}\right\}\frac{\partial\zeta_1}{\partial r}\,dr}{\int_0^1 (1-r)\sqrt{1+\beta^2\left(\frac{d\zeta_o}{dr}\right)^2}\,dr} \tag{12}$$

Thus, the heat release response can now be evaluated solving eq. together with eq. and using the result in eq. . Finally, noting that F_ϕ is identically zero in the present analysis, the heat release transfer function may be determined from eq. as follows,

$$F_u(St)=\frac{\int_0^1 (1-r)\left\{\beta^2\left(d\zeta_o/dr\right)\Big/\sqrt{1+\beta^2\left(d\zeta_o/dr\right)^2}\right\}\frac{\partial\hat{\zeta}_1}{\partial r}\,dr}{\int_0^1 (1-r)\sqrt{1+\beta^2\left(\frac{d\zeta_o}{dr}\right)^2}\,dr} \tag{13}$$

Where, the Strouhal number St is defined as: $St=\omega L_f/U_o$ and the caret on the RHS represents the Fourier transform w. r. t. t. Results for F_u developed by various groups can be recovered from the above formulation by appropriate choice of the excitation velocity shape functions: f_u, f_v and mean flame surface shape $\zeta_o(r)=r$ for inverted wedge flames. Results for conical flames can be obtained by the replacement, $r\to 1-r$ in eqs. (9) - (13). These results are now discussed in the following paragraphs.

The first comparison of transfer functions obtained from the above formulation with experimental measurements was obtained by Ducruix et al [4]. Their theoretical formulation can be recovered from the above by choosing, $f_u=0$, $f_v=\sin(St\,t)$ and $\zeta_o(r)=r$ and finally making the replacement $r\to 1-r$ in the above equations. The magnitude and phase of F_u obtained from their analysis were compared with corresponding experimental measurements of the same obtained from measurements of CH* chemiluminesence for an axis-symmetric and attached Bunsen flame. Measurements were obtained for two different excitation amplitudes and burner diameters over a range of mean flow velocities (see Ducruix et al [4] for details). These results are presented in fig. 6 as a function of a reduced Strouhal number which can be written in terms of the notation introduced above as: $\omega^*=St\left(1+\beta^2\right)/\beta^2$. It is clear that both magnitude and phase determined from theory are in reasonable upto an $\omega^*\approx 4$ in both cases shown in fig. 6.

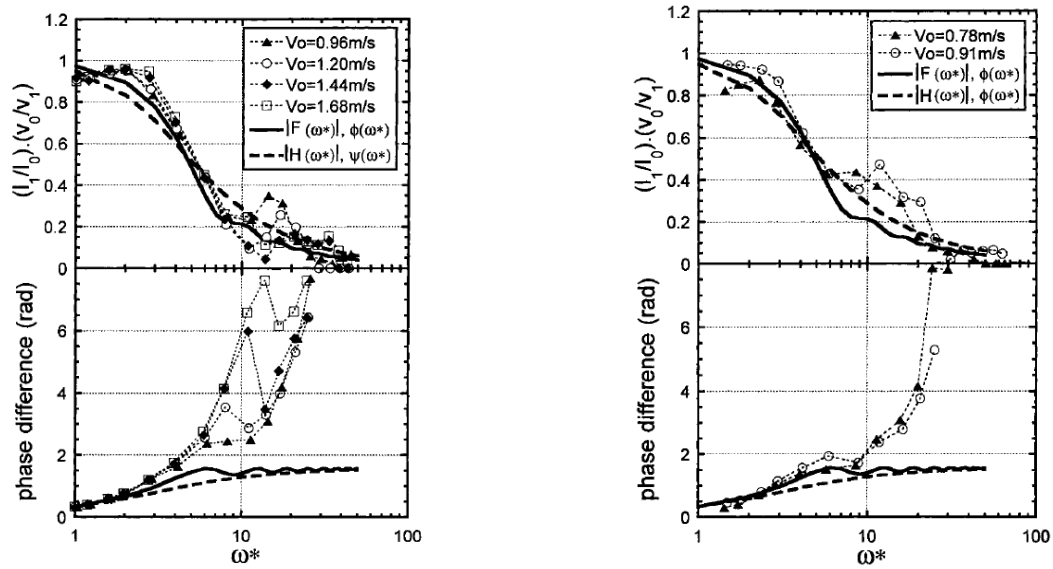

(a) (b)

Figure 6: Comparisons between theoretically determined and experimentally measured velocity coupled transfer functions from Ducruix et al [4]. for two excitation amplitude-burner diameter pairs (a) $u' = 0.192\,ms^{-1}$, D = 22mm and (b) $u' = 0.160\,ms^{-1}$, D = 30mm. The solid curve represents the theoretical prediction and the symbols are corresponding experimental values.

However, the theory predicts a saturating phase behavior for $\omega^* > 4$ which is at variance with the trend seen from experiments.

This issue was addressed in Schuller et al [5] for the case of the experimental setup used in refs. [4, 28] and further generalized by Preetham et al [6]. Schuller et al [5] extended the velocity field in the model of Ducruix et al [4] by assuming that velocity perturbations convect with the mean flow velocity field, i.e. by choosing $f_v = \sin\left(St\left(t - z\right)\right)$ in the above formulation and proceeding as in the case of Ducruix et al. [4] The physical reasoning for this choice is as follows. Several studies of axially forced jets have shown that velocity disturbances produced at the burner lip are convected downstream at a characteristic velocity. This characteristic velocity depends on a Strouhal number based on the forcing frequency, exit momentum thickness and mean flow velocity (refs). In Schuller et al [5], this velocity was shown to be equal to the flow velocity from PIV measurements on their setup. Thus, the comparison between the experimentally measured transfer function and the axially convected perturbation theory (called F_{CCO} in ref. [5]) is shown in fig. 7. Note that in this case, the agreement between modeling and theory is reasonable across the entire range of ω^*.

Thus, the results discussed in fig. 7 suggest that there are two parameters that control the characteristics of flame response. The first is the reduced Strouhal number ω^* and the second is the convection speed of the velocity perturbations induced by the shear layer instabilites in the presence of acoustic forcing. The characteristics of the instability waves that grow and merge to form these large scale peturbations are a function of the specific characteristics of the shear layer, such as co-flow velocity, and its sensitivity to external disturbances. In addition, the phase speed of the convected vortical instability waves are not equal to the flow velocity, but vary with frequency and shear layer characteristics. The instability wave growth rate similarly varies with

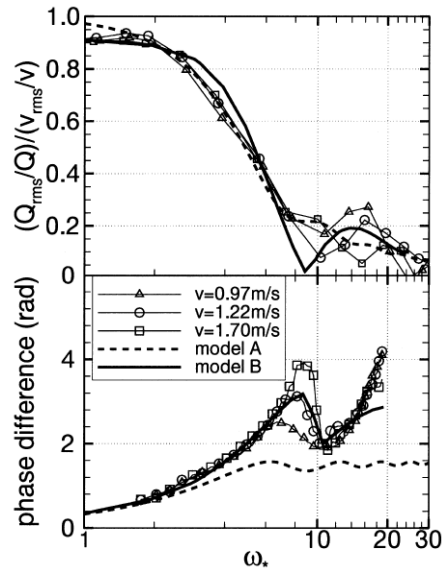

Figure 7: Comparisons between theoretically and experimentally measured velocity coupled transfer functions from Schuller et al. **[5]** Excitation amplitude $u' = 0.192\ ms^{-1}$, $D = 22\ mm$. The solid curve represents the theoretical prediction using the axially convected velocity model. The broken line is the result from Ducruix et al [4] and the symbols are corresponding experimental values.

frequency and the shear layer characteristics. For example, Michalke's [29] analysis of axially forced jets shows that the phase speed, u_c, of shear layer instability waves depend upon a momentum thickness (θ) based Strouhal number, $S_\theta = f\theta/u_\theta$ and dimensionless jet radius, R/θ. It shows that, for all R/θ values, the ratio of u_c/U_o equals unity and 0.5 for low and high Strouhal numbers. For thin boundary layers, e.g., R/θ = 100, the phase velocity actually exceeds the mean axial flow velocity in a certain S_θ range. This prediction has been experimentally verified as well. For example, Baillot et al. [30] measured u_c/U_o values of 1.13 and 1.02 at 35 and 70 Hz, respectively, on a conical Bunsen flame. Durox et al.[31] measured u_c/U_o = 0.5 values at 150 Hz in an axisymmetric wedge flame.

The above facts are captured in the modelling approach of Preetham et al [6] which can be recovered from the formulation in eqs. - by choosing, $f_u = 0$, $f_v = \cos\{St(t - Kz)\}$ and $\zeta_o(r) = r$ for an inverted wedge flame as shown in fig. 5. The parameter $K = U_o/u_c$. The resulting transfer function was found to be characterized by two parameters, a reduced Strouhal number St_2 identical to the corresponding parameter in the analyses of Ducruix et al **[4]** and Schuller et al. **[5]** and a new parameter, $\eta = K\{\beta^2/(1+\beta^2)\}$. Physically, the latter represents the time taken by a velocity perturbation to traverse the flame surface from base to tip normalized by the mean flow time over the same distance. The magnitude and phase of the transfer functions thus determined was found to be a strong function of this parameter for both conical and inverted wedge flames as shown by fig. 8 (note that Preetham et al use G to denote transfer functions). Although not shown here, the same strong dependence on η can be seen for the phase as well (see ref. [6]).

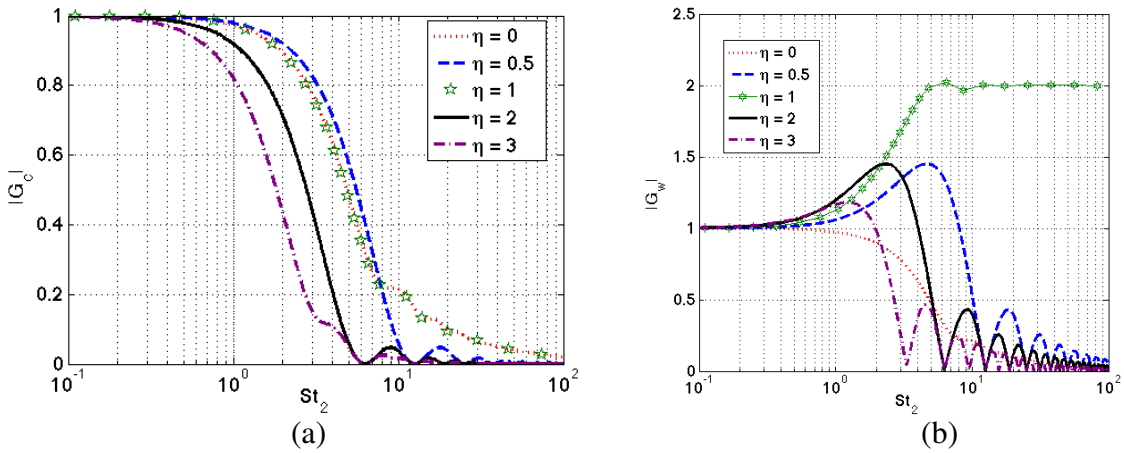

Figure 8: Variation of transfer function magnitude from the analysis of Preetham et al [6] (a) Conical flame and (b) inverted wedge flame. Note, in the notation of Preetham et al, the transfer function is denoted by *G* with the subscripts 'c' and 'w' denoting conical and wedge flames respectively.

An interesting feature of these transfer function is the presence of nodes, i.e. values of St_2 at which the flame response is identically zero *even* though the flame surface wrinkles in an unsteady fashion. Also, in the case of the wedge flame, the transfer function magnitude exceeds unity over a range of St_2 values for the $\eta > 0$ values presented in fig. 8. These features were first reported theoretically by Schuller et al **[5]** and measured experimentally by Durox et al. [31] Indeed, evidence of these features can be seen in the earlier experimental data from Ducruix et al [4] (e.g. fig. 6a for $10 < \omega^* < 11$) and Schuller et al **[5]** (e.g. fig. 7 for $\omega^* > 9$). These features are explained by the following analysis presented for the first time in Preetham et al. [6]. In general, the local flame surface slope is a superposition of two contributions. The first of these is due to spatial inhomogeneities in the perturbation velocity amplitude and the second, from the nature of the boundary condition at the attachment location. Mathematically, these two contributions correspond to the particular and homogeneous solutions respectively, of eq. (9). Each of these solutions yields a corresponding contribution to the net heat release transfer function. Thus,

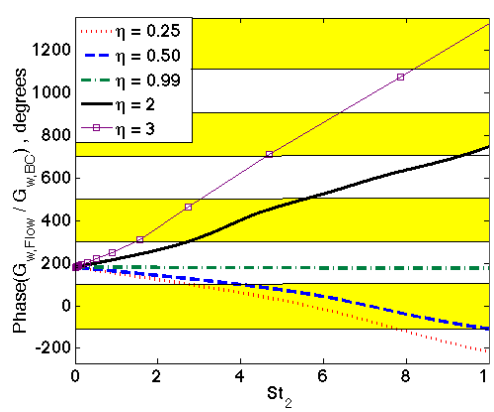

Figure 9: Phase difference between the contributions to the total transfer function from flow inhomogeneites and boundary conditions as shown in Preetham et al.[6] The yellow bands represent regions where these contributions are in phase.

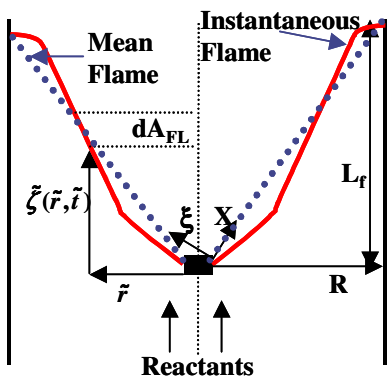

Figure 10: Schematic of the two-dimensional wedge flame geometry considered in the analysis of Preetham et al. [11] The broken line represents the mean location of the flame surface.

symbolically: $F\left(St_2\right)=F_{flow}\left(St_2\right)+F_{bndry}\left(St_2\right)$. These two contributions become successively in phase and out of phase relative to each other with increasing St_2 as shown by the result in fig. 9. Thus, this successive constructive and destructive interference between the two contributions results in the appearance of nodes and increase in the value of the transfer function magnitude above unity. Several other interesting results that elucidate the influence of non-linear flame kinematic processes in the limit of constant flame speed are presented in Preetham et al. [6].

All analyses discussed thus far have analyzed flame response in the limit of constant flame speed. As such, these analyses provide an understanding of heat release response processes due to the pathways shown in fig. 1. The next sub section discusses the influence of flame stretch on the above results.

3.1 INFLUENCE OF FLAME STRETCH

Initial theoretical analyses of the influence of flame stretch on heat release response have been performed by Wang et al [10] and Preetham et al. [11]. This section summarizes the results presented in the latter as it includes the results of the former within its framework. Both of the above papers analyze the response of a two dimensional wedge shaped flame subjected to acoustic forcing as shown schematically in fig. 10. The dependence of flame speed dependence on flame stretch can be decomposed into a dependence on flame front curvature and flow straining as shown in below,

$$s_L = s_{L,o}\left(1 - M_{a,c}\,C + M_{a,s}H\right) \tag{14}$$

Where, $s_{L,o}$ is the unstretched flame speed, $M_{a,c}$ is the Markstein length associated with curvature and $M_{a,s}$ is the Markstein length associated with hydrodynamic strain. The terms C and H are the curvature and hydrodynamic strain which can be written as below,

$$C = -\nabla \bullet \vec{n}$$

$$H = \frac{\vec{n} \bullet \nabla \times \left(\tilde{\vec{V}}\Big|_{\tilde{y}=\tilde{\zeta}} \times \vec{n} \right) - \left(\tilde{\vec{V}}_f \bullet \vec{n} \right)\left(\nabla \bullet \vec{n} \right)}{S_{L,o}} \tag{15}$$

The vector $\vec{n}$ is the normal vector pointing into reactants and $\tilde{\vec{V}}_f$ is the local speed of the flame front. Next, the heat release response now comprises of two contributions due to burning area oscillations and flame speed oscillations respectively as follows,

$$\frac{q'}{q_o} = \frac{A'}{A_o} + \frac{\int_{flame} s_L' dA_o}{\int_{flame} s_{L_o} dA_o} \tag{16}$$

Thus, following the analysis detailed in Preetham et al, the transfer function contributions in the limit of small $M_{a,c}/R$ and $M_{a,s}/R$ (R = duct radius, see fig. 5) can be written as follows,

$$\begin{aligned} G_{Area} &= i\frac{e^{iSt_2} - e^{i\eta St_2}}{(\eta-1)St_2} + \underbrace{\frac{\eta\left(e^{iSt_2} - e^{i\eta St_2}\right)}{(\eta-1)}\sigma_s^*}_{Hydrodynamic\ Strain} + \underbrace{\frac{\left(\eta^2 e^{i\eta St_2} - e^{iSt_2}\left((\eta-1)iSt_2 + \eta^2\right)\right)}{(\eta-1)^2}\sigma_c^*}_{Curvature} + O\left(\sigma^{*2}\right) \\ G_{SL} &= \underbrace{\left(e^{i\eta St_2} - 1\right)\sigma_s^*}_{Hydrodynamic\ Strain} + \underbrace{\frac{\left(\eta - 1 + e^{iSt_2} - \eta e^{i\eta St_2}\right)}{(\eta-1)}\sigma_c^*}_{Curvature} + O\left(\sigma^{*2}\right) \end{aligned} \tag{17}$$

Where the parameters $\sigma_c^* = M_{a,c}\Big/\left(R\beta\sqrt{1+\beta^2}\right)$ and $\sigma_s^* = M_{a,s}\beta\Big/\left(R\sqrt{1+\beta^2}\right)$ are scaled Markstein lengths. The result of Wang et al [10] may be obtained from the above by setting $M_{a,s} = 0$ and passing to the limit of a spatially constant velocity amplitude $(\eta \to 0)$. Consider first the expression for G_{Area}. Clearly, the hydrodynamic strain term becomes comparable to the first in magnitude when $\eta\sigma_s^* St_2 \sim 1$ and likewise, from the curvature term, when $\sigma_c^* \sim 2(\eta-1)\Big/\left(2St_2^2(\eta-1) - \eta^2 St_2\right)$. The latter, in the limit of spatially constant velocity perturbation magnitude yields $\sigma_c^* St_2^2 \sim 1$ as the criterion when the effect of stretch on flame surface kinematics has a significant effect on burning area. The former more general result however, has not been reported in Preetham et al [11] and therefore, merits further investigation. Finally, in the limit $\eta \to 0$ of the direct contribution becomes significant when $\sigma_c^* St_2 \sim 1$. Further results on the influence of flame stretch on heat release response may be found in Preetham et al [11] and Wang et al. [10].

3.2 INFLUENCE OF GAS EXPANSION

Theoretical analyses of the problem of the influence of gas expansion on heat release response are few and have been mainly restricted to addressing the question of turbulent flame speed and flame front instabilities. This problem is challenging to solve theoretically because of the complexity of having to capture the two-way coupling between the flame and the surrounding flow field. As such, it is not possible to proceed as before by specifying a perturbation velocity field. Mehta and Soteriou [32] have made an attempt to address this problem. However, the treatment of gas expansion effects is ad hoc and based on a number of restrictive assumptions. Hence, this problem remains a significant issue that needs to be addressed adequately by

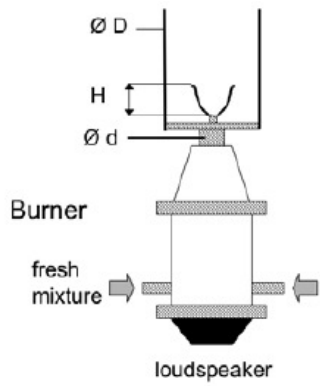

Figure 11: Schematic of the experimental setup used by Birbaud et al. [35] The flame is a inverted conical flame. This illustration was adapted from Birbaud et al. [35]

theoretical analyses. It must be noted that Wu et al [26] have presented a theoretical analysis of the problem studied experimentally by Searby [33] showed that under proper conditions, flame front instabilities can cause excitation of self-sustaining acoustic oscillations. However, a parallel analysis for the forced response case for an attached flame has yet not been presented to the best of the author's knowledge. Thus, efforts towards understanding of this problem have adopted a computational/experimental approach. Birbaud et al [34] showed that gas expansion effects cause the unsteady motions in the upstream flow of fresh reactants to change from convective type disturbances to acoustic type disturbances with changing excitation frequency. This fact can be conceptualized in terms of the parameters presented in the previous sections as a change in the parameter η with increasing frequency.

Further, a different set of experiments by Birbaud et al also show a strong influence of confinement on the heat release transfer function of a ducted inverted conical flame. Their setup is shown schematically in fig. 11. Heat release transfer functions were determined from global CH* chemiluminesence emissions from the flame. Further details on the experimental techniques

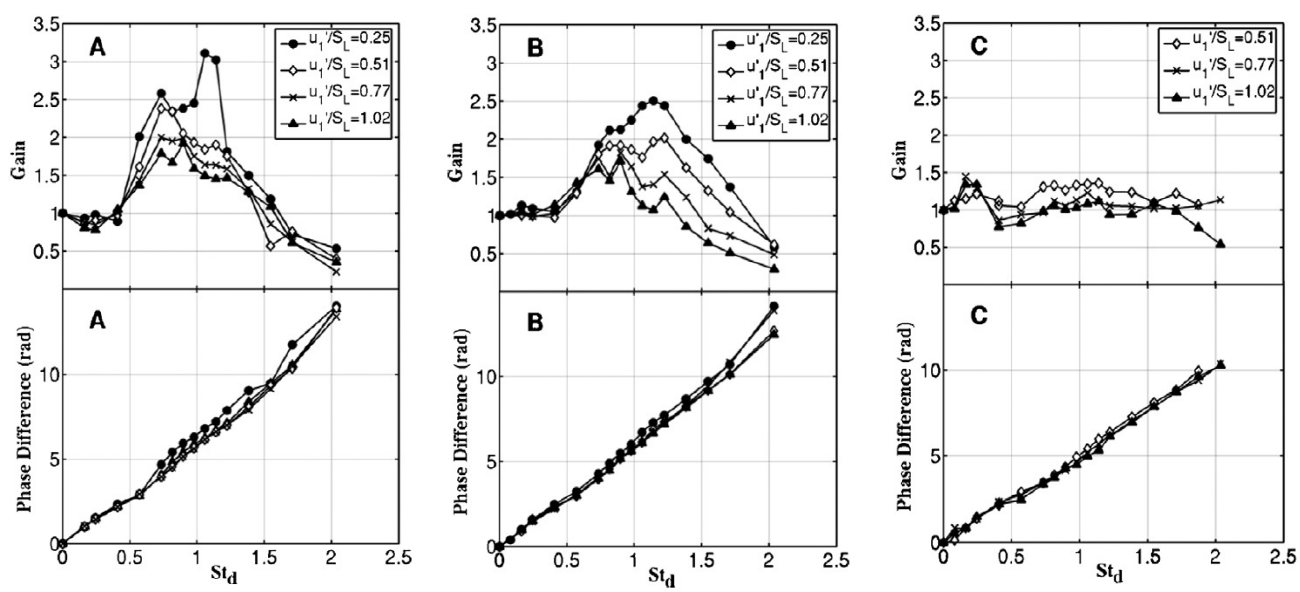

Figure 12: Experimentally determined transfer functions for confined wedge flames from Birbaud et al. [35]. U_o=2.7ms^{-1} and equiv. ratio is 1.03 in all cases. St_d is the Strouhal number based on inlet diameter *d* (see fig. 11). The confinement ratio *d/D* is given by (A) 0 (unconfined) (B) 0.32 (C) 0.64.

used may be found in their original paper. Figure 12 shows the magnitude and phase of the measured transfer functions as a function of a Strouhal number based on inlet duct diameter *d* (see fig. 11). The confinement ratio, *d*/*D*, is varied from 0 in Case A to 0.64 in case C. Note that the transfer function gain at all values of St_d decrease with increasing *d*/*D* values showing clearly that confinement significantly influences heat release response. Note however, that even though the length of the outer duct was chosen such that the range of excitation frequencies in the experiment was well below the fundamental quarter wave mode in order to avoid resonances, it is impossible to avoid the effect of acoustic feedback on the flame due to reflections at the duct exit plane. Even so, the amplitude of such reflected waves would scale with the imposed forcing amplitude and hence can be expected to be small for the cases presented here. Similar trends can be seen in the recent experiments of Karimi et al [36], conducted on a ducted conical flame.

Preetham et al [37] performed computations of a two ducted flame using a level-set based Ghost fluid Method coupled with an Euler solver to capture full two way coupling between the flame and the flow. They postulated that the main influence of thermal expansion is to introduce spatial inhomogeneity in the local mean flow velocity tangential to the unforced mean flame surface and the amplitude of the perturbation velocity component normal to the mean flame surface. An effective Strouhal number and reference velocity, motivated from a generalization of the analysis presented at the beginning of this section to include effects of mean flow inhomogeneites were determined from the obtained computational results. Transfer functions determined using these parameters from the results presented in Preetham et al [37] showed good agreement with computations for the magnitude. The phase reduction was found to be problematic for reasons specific to the case analyzed in the paper (see ref. for details).

As such, following the above analysis, the effective Strouhal number can be defined as the ratio of the effective transit time of flame wrinkles along the flame surface normalized by the acoustic time period. The upstream equivalence ratio and nominal mean flow velocity were held constant at 1.03 and 2.7 ms^{-1} for each of the confinement ratios studied in Birbaud et al. [35]. As such, with increasing confinement ratio, the acceleration of the mean flow due to gas expansion across the flame front increases. Hence, the effective transit time of wrinkles on the flame surface is reduced causing the effective St_d to reduce from its nominal value as shown on the horizontal axis of each result shown in fig. 12. Thus, the response of the flame appears to move towards the quasi-steady limit with increasing confinement ratio as borne out by the nearly unity transfer function magnitude in fig. 12c.

Finally, the influence of hydrodynamic instability on the transfer function was studied for a two-dimensional ducted flame in a recent paper by Hartmann et al.[12]. Hydrodynamic instability causes wrinkles of wavelengths greater than a lower cutoff to increase in amplitude due to coupling between flame surface motions and velocity perturbations. The flame speed was assumed to depend on curvature alone (i.e. by setting $M_{a,s} = 0$ (see eq.(14))) in these simulations. Hence, for a given disturbance wavelength, there is a value of $M_{a,c}$ which makes the flame neutrally stable to perturbations. It was shown that the net heat release response is completely dominated by the response of the flame area in the case of hydrodynamically unstable flames. The direct stretch response was also found to occur at much lower frequencies than predicted by the theoretical limits presented earlier.

4 FUEL/AIR RATIO COUPLED RESPONSE

Much analytical insight into this problem can be obtained from the simple time delay analysis that treats the flame as a concentrated heat release source [38]. However, in general, flames are

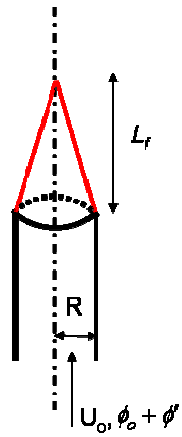

Figure 13: Schematic of investigated geometry from Hemchandra et al.[9]

convectively non-compact with respect to fuel-air ratio fluctuations, i.e. the length scale of the fuel-air ratio oscillations is smaller than the global flame length, requiring therefore, a detailed flame kinematic analysis as was discussed in the previous section. This mechanism has been studied by several groups in the past, analytically [8, 9, 39] and through computations[40]. However, detailed reduced order modeling efforts in order to understand the influence of various pathways that cause the heat release of the flame to oscillate as a result of this mechanism are relatively few. This section will review the modeling approach of Hemchandra et al [9] which is similar to the previously developed model of Cho and Lieuwen [8]. An additional effect due to non-quasi steady flame speed response caused the finite time delay required for fuel/air ratio fluctuations to diffuse past the preheat zone of the flame have been analyzed [24] and incorporated into the original formulation in Hemchandra et al [9] will also be reviewed.

Fundamentally, equivalence ratio oscillations are caused due to two reasons. An oscillating pressure drop across a fuel injector upstream of the combustion zone can cause the mass flow rate of fuel through the injector to oscillate if the fuel injector is not choked. Alternatively, pressure oscillations can cause the air mass flow rate at the fuel injector to oscillate causing the resultant fuel/air ratio to change even if the fuel injector is choked. Once generated, these fuel/air ratio perturbations advect with the mean flow into the combustion zone causing heat release oscillations. Hemchandra et al [9]analyzed the influence of fuel air ratio oscillations on heat release for conical Bunsen flames as shown in fig. 13, subject to harmonic perturbations in upstream equivalence ratio of the form $\phi(t) = \phi_o\left\{1+\varepsilon\cos\left[St\left(t-z\right)\right]\right\}$. Thus, defining $G(r,z,t) = z - \zeta(r,t)$ as before yields the following kinematic equation for the instantaneous flame surface position (in non-dimensional form).

$$\frac{\partial\zeta}{\partial t} + f(\phi)\sqrt{\frac{1+\beta^2\left(\partial\zeta/\partial r\right)^2}{1+\beta^2}} = 1 \tag{18}$$

Where, ϕ is the instantaneous local equivalence ratio of the unburnt mixture and the function $f(\phi) = s_L(\phi)/s_{Lo}$ (s_{Lo} = laminar flame speed at ϕ_o). All other symbols have the same definition as presented in the previous section unless otherwise specified. As in the case of velocity coupled oscillations, the function $\zeta(r,t)$ is written as a asymptotic series in ε as:

$\zeta(r,t) = 1 - r + \varepsilon\zeta_1(r,t) + O(\varepsilon^2)$. Hemchandra et al [9] present the solution upto the third order term of the above series. These solutions at each order in ε depend on the sensitivities of local flame speed and heat of reaction terms defined as below,

$$s_{Lj} = \frac{1}{j!}\frac{\partial^j f(\phi)}{\partial(\phi'/\phi_0)^j}\bigg|_{(\phi'/\phi_0)=0} ; \qquad h_{Rj} = \frac{1}{j!}\frac{\partial^j (h_R/h_{R0})}{\partial(\phi'/\phi_0)^j}\bigg|_{(\phi'/\phi_0)=0} \tag{19}$$

Results for the transfer function at leading order in ε were obtained using the following curve fits for s_L and h_R (dimensional form),

$$\begin{aligned} s_L(\phi) &= A\phi^B e^{-C(\phi-D)^2}; \quad A = 0.6079,\ B = -2.554,\ C = 7.31,\ D = 1.230 \\ h_R(\phi) &= \frac{2.9125\times10^6 \min(1,\phi)}{1+0.05825\phi} \end{aligned} \tag{20}$$

As discussed earlier, overall heat release transfer function can be decomposed into individual contributions from burning area response, flame speed response and heat of reaction response. Expressions for these contributions have been determined in Hemchandra et al [9] as follows,

Burning area:

$$F_{o,A} = s_{L_1}\left\{\frac{2\alpha}{1-\alpha}\left(\frac{1-\alpha-\exp(iSt)+\alpha\exp\left(iSt/\alpha\right)}{St^2}\right)\right\} \qquad \alpha = \frac{\beta^2}{1+\beta^2} \tag{21}$$

Flame speed:

$$F_{o,s_L} = s_{L1}\left\{\frac{2}{St^2}\left(1+iSt-\exp(iSt)\right)\right\} \tag{22}$$

Heat of reaction:

$$F_{o,h_R} = h_{R1}\left\{\frac{2}{St^2}\left(1+iSt-\exp(iSt)\right)\right\} \tag{23}$$

Note first that it clear from the above that the magnitude of F_{o,s_L} and F_{o,h_R} is controlled by the value of the flame speed and heat of reaction sensitivity to equivalence ratio fluctuations. Also, since area variations in the present case are caused purely due to unsteady spatial variations in s_L, the $F_{o,A}$ contribution scales as s_{L1} as well.

The variation of each of the above contributions and the total transfer function with reduced Strouhal number St_2 is presented in fig. 14 for $\phi_o = 0.85$ and 1.227. These values were chosen so that the mean flame shape in both cases is the same and as such, their response characteristics can be compared. Note first that the overall transfer function shows a non-monotonic variation with St_2 due to the fact that it is a superposition of contributions with varying magnitudes and phases relative to each other. For the lean case, the transfer function tends to the value of F_{o,h_R} in the limit of $St_2 \to 0$ as the $F_{o,A}$ and F_{o,s_L} become equal in magnitude but opposite in phase in this limit (see fig. 14). Physically, in the quasi-steady limit, the change in flame area is negatively

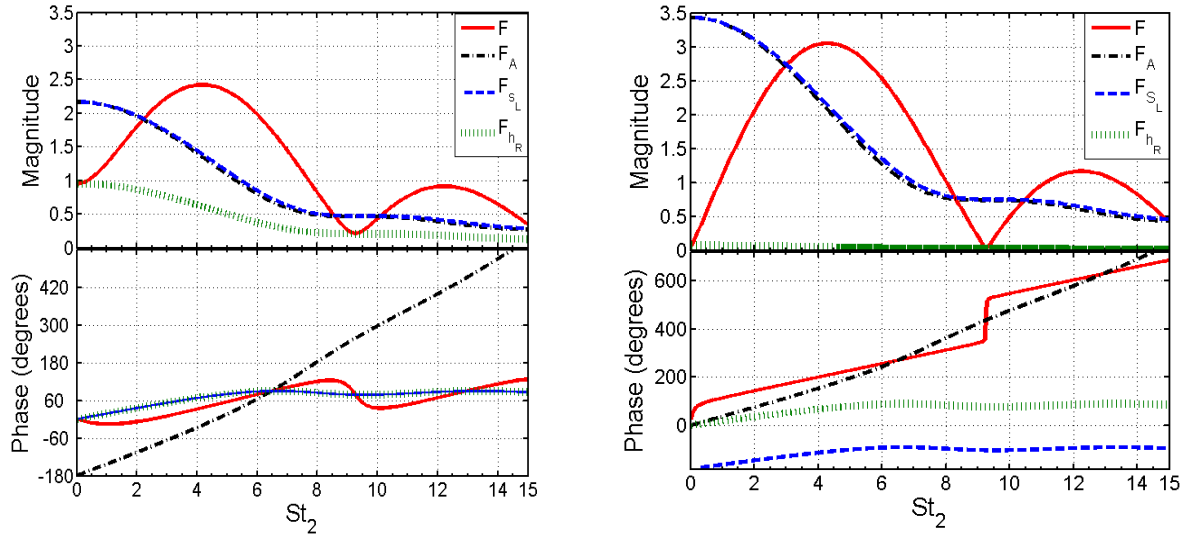

(a) (b)

Figure 14: Linear transfer function of a) $\phi_o = 0.85$ (lean) b) $\phi_o = 1.277$ (rich). $\beta = 4$ as presented in Hemchandra et al.[9]

correlated with an increase in flame speed as the latter causes the flame to burn into fresh reactants at a faster rate. This fact is reflected in the mathematics of the present model as the balance between the corresponding transfer function contributions. The same occurs for the rich equivalence ratio as well. However, in this case the contribution from F_{o,h_R} is very small as the heat of reaction sensitivity h_{R1} is very small on the rich side. Hence, the net response in the rich case vanishes in the quasi-steady limit. Note also, that this allows for the appearance of nodes in the net response for the rich flame. Thus, it is clear that the stability characteristics (i.e. unstable frequencies, limit cycle amplitudes etc.) for combustors lean flames will be different from those with rich flames even if the nominal flame shape characteristics are the same.

The formulation presented in Hemchandra et al. [9] assumes that the local flame speed responds to local fluctuations in equivalence ratio in a quasi-steady manner. However, this is not strictly true as has been shown by a detailed study of flame speed response to equivalence ratio fluctuations for a 1D premixed flame using a detailed chemical reaction mechanism [41]. A detailed analysis of non-quasisteady effects on flame response may be found in Shreekrishna et al. [24] These non quasi-steady effects are controlled by a new Strouhal number defines as: $St_\delta = \omega\delta / s_L$. This Strouhal number is essentially the ratio of the time taken for an equivalence ratio disturbance to diffuse through the preheat zone of thickness δ and the acoustic time period. Thus, the non-quasisteady counterparts of each of the transfer function contributions presented in eqs. (21)-(23) can be determined from the following using the following formula,

$$F^{nqs} = g\left(St_\delta\right) F^{qs}\left(St\right) \tag{24}$$

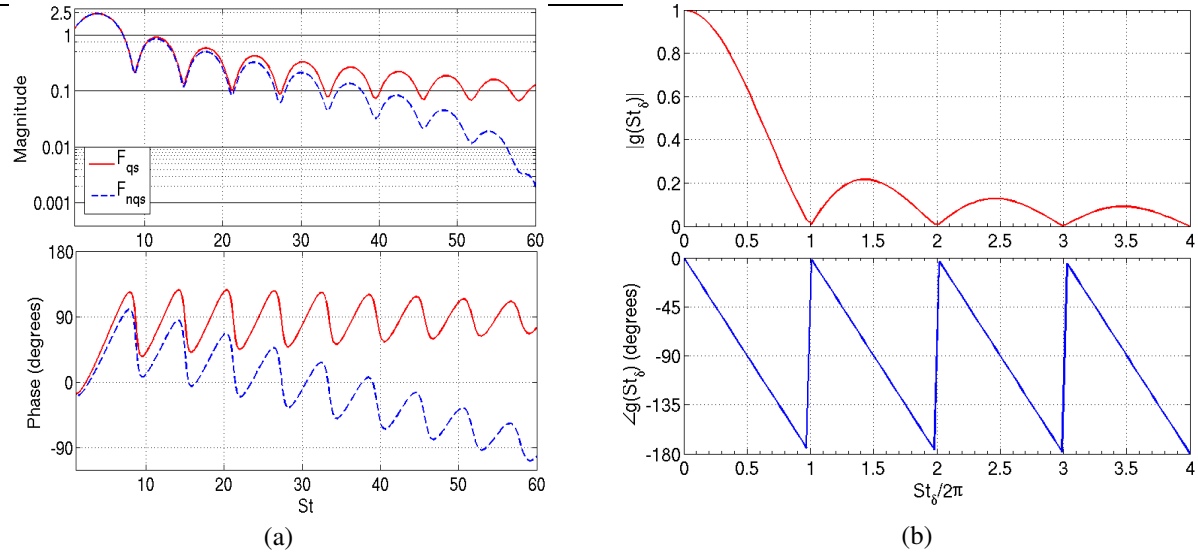

Figure 15: (a) Non quasi-steady versus quasi-steady flame response for $\phi_o = 0.85$, $\beta = 4$, $\delta = 0.1R$ (b) Non quasi-steady correction factor as presented in Shreekrishna et al. [24]

Where, $g\left(St_\delta\right) = \mathrm{sinc}\left(St_\delta/2\right)\mathrm{e}^{-iSt_\delta/2}$ and F^{qs} are the corresponding transfer functions presented in eqs. (21)-(23). Figure 15a compares the magnitude and phase of the linear total transfer function for quasi-steady and non quasi-steady flame response. It is clear that the non-quasi-steady response deviates significantly from the corresponding quasi-steady result. In fact, it may be observed from fig. 15b, that at $St_\delta \sim \pi$, there is already about 40% attenuation in the gain, and 90 degrees difference in phase with respect to the quasi-steady response. As discussed in Shreekrishna et al. [24] for a methane-air reactant mixture and a tall flame ($\beta = 10$), the preheat zone thickness is ~ 1 mm at 1 atm. Thus, at 1 atm, the flame preheat zone diffusive processes become non quasi-steady at a frequency f~400 Hz. However at 10 atm, typical of operating pressures in gas turbine engines, the preheat zone becomes non quasi-steady at f~4 kHz. As such, the extent to which non-quasisteady effects play a role in influencing heat release response in gas turbine combustors is as yet unclear. The above estimate suggests that these effects might become significant during the course of high frequency instabilities.

5 CONCLUSION

The present paper presents a brief overview of advances in modelling the heat release response of premixed flames to perturbations in flow velocity and fuel air ratio over the past decade. Current analytical modeling approaches are based on the G-equation approach. This approach assumes that the flame is a thin boundary separating reactants from products. In the interest of obtaining physical insight into the various processes that control the characteristics of heat release response, theoretical approaches neglect the effect of gas expansion across the flame surface.

The net response to flow velocity oscillations (velocity coupled response) was shown to be the superposition of individual contributions arising from spatial variation in the perturbation velocity field and the nature of flame attachment. It was shown that this results in the heat release response magnitude having a non-monotonic dependence on the excitation frequency. Further, conditions under which flame stretch effects become important have been determined. A detailed analysis of the response of the flame to fluctuations in fuel/air ratio have also been developed. It

was shown that rich and lean flames have fundamentally different response characteristics due to the difference in the nature of the sensitivity of flame speed and heat of reactions to fluctuations in equivalence ratio at rich and lean mean equivalence ratios. The effect of mass diffusion induced non-quasisteady effects has also been determined.

While the above modeling efforts have yielded valuable physical insight into the various physical mechanisms affecting heat release response, several important issues remain to be addressed. Although not reviewed in the present paper, the presence of background turbulence has been shown to quantitatively change the characteristics of flame response. This may be conceptualized as being due to a modulation of turbulent consumption speed in te presence of acoustic forcing. Further work is essential to understand this effect even in the zero gas expansion limit.

A second important issue is the influence of flame front instabilities on flame surface response. This is a phenomenon that depends on the presence of gas expansion for its existence and as such cannot be captured by any analysis that ignores the same. However, preliminary computational investigations have shown that it is a significant factor influencing flame surface response and as such merits further analytical study in order to elucidate it's role in influencing the response of premixed flames to flow field perturbations.

6 ACKNOWLEGDEMENTS

The support for this work received from the Deutsche ForschungsGemeinschaft (DFG) through the collaborative research center SFB 686 is gratefully acknowledged.

REFERENCES

[1] Mcmanus, K. R., Poinsot, T. and Candel, S. M., "A review of active control of combustion instabilities", Progress in Energy and Combustion Science 19 (1) (1993) 1-29.

[2] Dowling, A., "A kinematic model of a ducted flame", Journal of Fluid Mechanics 394 (1999) 51-72.

[3] Fleifil, M., Annaswamy, A. M., Ghoneim, Z. A. and Ghoniem, A. F., "Response of a laminar premixed flame to flow oscillations: A kinematic model and thermoacoustic instability results", Combustion and Flame 106 (4) (1996) 487-510.

[4] Ducruix, S., Durox, D. and Candel, S., "Theoretical and Experimental Determinations of the Transfer Function of a Laminar Premixed Flame", Proceeding of the Combustion Institute 28 (1) (2000) 765-774.

[5] Schuller, T., Durox, D. and Candel, S., "A unified model for the prediction of laminar flame transfer functions comparisons between conical and V-flame dynamics", Combustion and Flame 134 (1-2) (2003) 21-34.

[6] Preetham, Hemchandra, S. and Lieuwen, T. C., "Dynamics of Laminar Premixed Flames Forced by Harmonic Velocity Disturbances", Journal of Propulsion and Power 24 (6) (2008) 1390-1402.

[7] T. Schuller, D. D., S. Candel, "Dynamics of and Noise Radiated by a Perturbed Impinging Premixed Jet Flame", Combustion and Flame 128 (2002) 88-110.

[8] Cho, J. H. and Lieuwen, T., "Laminar Premixed Flame Response to Equivalence Ratio Oscillations", Combustion and Flame 140 (2004) 116-129.

[9] Hemchandra, S., Shreekrishna and Lieuwen, T., "Premixed flame response to equivalence ratio perturbations", ASME/ASEE/AIAA Joint Propulsion Conference, Cincinnati OH, 2007, AIAA 2007-5656.

[10] H. Y. Wang, C. K. Law and Lieuwen, T., "Linear response of stretch-affected premixed flames to flow oscillations", Combustion and Flame 156 (2009) 889-895.

[11] Preetham, Thumuluru, S. K., Hemchandra, S. and Lieuwen, T., "Linear Response of Laminar Premixed Flames to Flow Oscillations: Unsteady Stretch Effects ", Journal of propulsion and power, to appear (2010)

[12] Hartmann, D., Schroeder, W. and Hemchandra, S., "Influence of hydrodynamic instability of the response of acoustically forced premixed flames", ASME Turbo EXPO Glasgow, UK, 2010, GT2010-22848.

[13] Bellows, B. D., Hreiz, A. and Lieuwen, T., "Nonlinear Interactions between Driven and Self-Excited Acoustic Oscillations in a Premixed Combustor", (2006)

[14] Balachandran, R., Ayoola, B. O., Kaminski, C. F., Dowling, A. P. and Mastorakos, E., "Experimental investigation of the nonlinear response of turbulent premixed flames to imposed inlet velocity oscillations", Combustion and Flame 143 (1-2) (2005) 37-55.

[15] Peters, N., Turbulent Combustion, Cambridge University Press, Cambridge, UK, 2000.

[16] V. Moreau, B. Fiorina and Pitsch, H., "A level set formulation for premixed combustion LES considering the turbulent flame structure", Combustion and Flame 156 (2009) 801-812.

[17] Matalon, M. and Matkowsky, B. J., "Flames as gasdynamic discontinuities", Journal of Fluid Mechanics 124 (1982) 239-259.

[18] Clanet, C., Searby, G. and Clavin, P., "Primary acoustic instability of flames propagating in tubes: cases of spray and premixed gas combustion", Journal of Fluid Mechanics 385 (1999) 157-197.

[19] Mcintosh, A. C., "Pressure disturbances of different length scales interacting with conventional flames", Combustion Science and Technology 75 (4-6) (1991) 287-309.

[20] Mcintosh, A. C., "The linearised response of the mass burning rate of a premixed flame to rapid pressure changes", Combustion Science and Technology 91 (4) (1993) 329-346.

[21] Peters, N. and Ludford, G. S. S., "The effect of pressure variations on premixed flames", Combustion Science and Technology 34 (1) (1983) 331-344.

[22] Shanbhogue, S. J., Plaks, D. V. and Lieuwen, T., "The KH Instability of Reacting, Acoustically Excited Bluff-Body Shear Layers", 43 rd AIAA/ASME/SAE/ASEE Joint Propulsion Conference, 2007, AIAA #2007-5680.

[23] Hemchandra, S., Shreekrishna and Lieuwen, T., "Premixed flame response to equivalence ratio perturbations", AIAA/ASME/ASEE Joint propulsion conference, Cincinnati, OH, 2007, AIAA# 2007-5656.

[24] Shreekrishna, Hemchandra, S. and Lieuwen, T., "Premixed flame response to equivalence ratio perturbations", Combustion Theory and Modelling (submitted)

[25] Shreekrishna and Lieuwen, T., "High frequency premixed flame response to acoustic perturbations", 15th AIAA/CEAS Aeroacoustics conference, Miami, FL, 2009, AIAA-2009-3261.

[26] Wu, X., Wang, M., Moin, P. and Peters, N., "Combustion instability due to the nonlinear interaction between sound and flame", Journal of Fluid Mechanics 497 (2003) 23-53.

[27] Hemchandra, S., Peters, N. and Lieuwen, T., "Heat release response of acoustically forced turbulent premixed flames – role of kinematic restoration", 33rd Internatonal Symposium on Combustion (submitted) (2010)

[28] Schuller, T., Ducruix, S., Durox, D. and Candel, S., "Modeling tools for the prediction of premixed flame transfer functions", Proceedings of the Combustion Institute 29 (1) (2002) 107-113.

[29] Michalke, A., "Instability of a Compressible Circular Jet Considering the Influence of the Thickness of the Jet Boundary Layer", Zeitschrift fur Flug Wissenschaft 19 (1971)

[30] Baillot, F., Durox, D. and Prud'homme, R., "Experimental and theoretical study of a premixed vibrating flame", Combustion and Flame 88 (2) (1992) 149-152.

[31] Durox, D., Schuller, T. and Candel, S., "Combustion dynamics of inverted conical flames", Proceedings of the Combustion Institute 30 (2) (2005) 1717-1724.

[32] Mehta, P., Soteriou, M. and Banaszuk, A., "Impact of exothermicity on steady and linearized response of a premixed ducted flame", Combustion and Flame 141 (4) (2005) 392-405.

[33] Searby, G., "Acoustic instability in premixed flames", Combustion Science and Technology 81 (4) (1992) 221-231.

[34] Birbaud, A. L., Durox, D. and Candel, S., "Upstream flow dynamics of a laminar premixed conical flame submitted to acoustic modulations", Combustion and Flame 146 (2006) 541-552.

[35] Birbaud, A. L., Durox, D., Ducruix, S. and Candel, S., "Dynamics of confined premixed flames submitted to upstream acoustic modulations", Proceeding of the Combustion Institute 31 (2007) 1257-1265.

[36] Karimi, N., Brear, M. J., Jin, S. H. and Monty, J. P., "Linear and non-linear forced response of a conical, ducted, laminar premixed flame", Combustion and Flame 156 (11) (2009) 2201-2212.

[37] Preetham, Hemchandra, S. and Lieuwen, T., "Forced response of premixed flames: effect of flow non-uniformities", 43rd AIAA Aerospace Sciences Meeting, Reno, NV 2008, AIAA 2009-978.

[38] Dowling, A. P., "Thermoacoustic instability", 6th International congress on Sound and Vibration, 1999,

[39] Keller, J. J., Egli, W. and Hellat, J., "Thermally induced low-frequency oscillations", Zeitschrift für Angewandte Mathematik und Physik (ZAMP) 36 (2) (1985) 250-274.

[40] C. Angelberger, D. V., F. Egolfopoulos, "LES of Chemical and Acoustic Forcing of a Premixed Dump Combustor", Flow, Turbulence and Combustion 65 (2000) 205-222.

[41] Lauvergne, R. and Egolfopoulos, F. N., "Unsteady response of C3H3/Air laminar premixed flames submitted to mixture composition oscillations", Proceedings of the Combustion Institute 28 (2) (2000) 1841-1850.